JUSAN SCIENCE

Journal of Engineering and Environmental Systems

ISSN (Print): 3135-2510; ISSN (Online): 3135-2529

journal homepage: https://jusanscience.com/journals/jees

Research Article

Structure–Property Relationship of Ester-Functionalized and Hydrolyzed ProDOT Polymers for Electrochromic Applications

Alina Tilekkabylova[1], Sanzhar Abish[2], Adil Zulkarnayev[1], Dana Kanzhigitova[3,*], Mirat Karibayev[3], Salimgerey Adilov[2]

[1]Department of Chemical and Materials Engineering, Nazarbayev University, Astana, 010000, Kazakhstan
[2]Department of Chemistry, School of Sciences and Humanities, Nazarbayev University, Astana, 010000, Kazakhstan
[3]Renewable Energy Lab, National Laboratory Astana, Astana, 010000, Kazakhstan.

[*]Corresponding author: Dana Kanzhigitova, dana.kanzhigitova@nu.edu.kz

https://doi.org/10.66973/jees.26.008

Article info:

Received: 18 May 2026 / Revised: 07 June 2026 / Accepted: 09 June 2026 / Published: 10 June 2026

Tilekkabylova A., Abish S., Zulkarnayev A., Kanzhigitova D., Karibayev M., Adilov S. (2026). Structure–Property Relationship of Ester-Functionalized and Hydrolyzed ProDOT Polymers for Electrochromic Applications. *Journal of Engineering and Environmental Systems*, *1*(1), 98–110. https://doi.org/10.66973/jees.26.008

Abstract: This work investigates how post-synthetic hydrolysis of the ester-containing 2-ethylhexyl ester (EHE) side chains of PProDOT(EHE) affects the surface composition, electronic structure, and electrochromic properties of the hydroxylated derivative PProDOT(OH). Structural and surface analyses confirmed that hydrolysis modifies the side-chain functionality while preserving the ProDOT-based conjugated backbone. XPS analysis showed changes in the sulfur chemical environment after hydrolysis, including a decrease in neutral thiophene sulfur and an increase in the high-binding-energy sulfur component, which may be related to surface oxidation, residual post-treatment species, or fitting-related effects. Tauc analysis showed that the optical band gap decreases from 1.64 to 1.43 eV after hydrolysis. UPS analysis revealed a decrease in the work function and photoemission onset energy from 4.70 and 1.20 eV to 4.31 and 0.88 eV, respectively, with HOMO/LUMO levels shifting from −5.90/−4.26 eV to −5.19/−3.76 eV. These changes indicate easier oxidation of the hydrolyzed polymer. Spectroelectrochemical measurements at −2.0/+2.0 V showed reversible electrochromic behavior, with decreased visible π–π* absorption and increased long-wavelength absorption upon oxidation. Cyclic voltammetry at 25–500 mV s^{-1} confirmed the retained redox activity of both polymers, although PProDOT-OH showed a lower current response. At the device level, hydrolysis accelerates switching, with Tc/Tb values of 0.28/0.25 s compared with 0.60/0.35 s for PProDOT-EHE but decreases optical contrast and coloration efficiency from 61.99% and 872.2 cm^2 C^{-1} to 43.41% and 599 cm^2 C^{-1}, respectively. Therefore, hydrolysis provides an effective route for tuning the balance between switching speed, optical contrast, and electronic structure in ProDOT-based electrochromic polymers.

Keywords: PProDOT-based polymer; conducting polymer; electrochromism; hydrolysis; side-chain engineering; optical switching; coloration efficiency.

https://doi.org/10.66973/jees.26.008

1 Introduction

Electrochromic materials are capable of reversibly changing their optical properties under an applied electrical potential, making them attractive for smart windows, low-power displays, adaptive camouflage, optical shutters, energy-saving glazing, and wearable optoelectronic devices[1], [2], [3]. The electrochromic effect is generally associated with reversible redox processes, where charge injection and extraction alter the electronic structure of the active material and produce changes in color, transparency, or near-infrared absorption[4], [5]. An ideal electrochromic material should exhibit high optical contrast, fast switching time, good coloration efficiency, long-term cycling stability, low operating voltage, and compatibility with flexible or solution-processable device architectures[6], [7].

Among different classes of electrochromic materials, conducting polymers have attracted particular attention because their molecular structures can be rationally designed to tune, morphology, and film-forming behavior[8], [9], [10]. Compared with inorganic electrochromic oxides, conducting polymers often offer faster switching kinetics, easier processing, mechanical flexibility, and the possibility of large-area fabrication by spin coating, spray coating, printing, or electropolymerization[11], [12]. Their optical properties can be controlled by modifying the conjugated backbone, introducing donor–acceptor motifs, changing side-chain architecture, or using post-polymerization chemical treatments[13], [14].

Polythiophene derivatives are among the most widely studied conducting polymers for electrochromic applications due to their relatively high environmental stability, tunable electronic structure, and reversible p-doping/dedoping behavior[15], [16]. Poly(3,4-ethylenedioxythiophene) and related poly(3,4-alkylenedioxythiophene) derivatives have become important electrochromic systems because of their low oxidation potentials, stable doped states, and strong optical modulation between neutral and oxidized forms[17], [18]. The presence of electron-rich dioxythiophene units lowers the oxidation potential and promotes the formation of stable charge carriers, such as polarons and bipolarons, during electrochemical oxidation[19], [20].

Poly(3,4-propylenedioxythiophene), commonly known as ProDOT-based polymers, provides an especially useful platform for structural modification because the propylenedioxy bridge can be functionalized with different side chains[21], [22], [23], [24]. Through side-chain engineering, the solubility, processability, intermolecular packing, surface morphology, electrolyte compatibility, and ion-transport behavior of ProDOT polymers can be adjusted without significantly disrupting the electroactive conjugated backbone. Bulky alkyl or branched side chains can improve solubility and film uniformity, while polar functional groups can enhance interaction with electrolytes and influence electrochemical switching. Therefore, the design of functionalized ProDOT polymers is an effective approach for balancing optical contrast, switching speed, coloration efficiency, and device stability[25], [26].

Post-polymerization modification is another powerful strategy for tuning conducting polymer properties. Unlike direct synthesis of multiple monomers, post-polymerization transformation allows chemical modification of side chains after polymer formation while maintaining the same conjugated backbone[27], [28]. In electrochromic polymers, this approach is particularly useful because small changes in side-chain polarity, hydrogen bonding, and ion-accessibility can strongly affect film morphology and redox kinetics. Hydrolysis of ester-containing side chains into hydroxyl-containing groups is one such transformation that can increase polarity and modify intermolecular interactions. However, the influence of ester-to-hydroxyl side-chain conversion on the optoelectronic and electrochromic behavior of ProDOT-based polymers remains insufficiently explored[29], [30].

In this work, we report the synthesis and electrochromic investigation of an ester-functionalized ProDOT-based polymer, PProDOT(EHE), and its hydrolyzed derivative, PProDOT(OH). The main objective is to understand how side-chain hydrolysis affects the chemical structure, electronic energy levels, electrochemical activity, and electrochromic device performance of ProDOT-based conducting polymers. The polymers were characterized by FTIR, XPS, UV–Vis spectroscopy, UPS, cyclic voltammetry, and

https://doi.org/10.66973/jees.26.008

electrochromic switching measurements. Electrochromic devices were assembled using a PMMA-based gel electrolyte, and their optical contrast, switching time, coloration efficiency, and cycling response were evaluated. The results reveal that hydrolysis narrows the optical band gap, shifts the frontier energy levels, modifies the sulfur and carbon chemical environments, and improves switching kinetics. This study demonstrates that side-chain hydrolysis is a simple but effective strategy for tuning the structure–property relationship of ProDOT-based electrochromic polymers.

2 Materials and Methods

Materials

3,4-Dimethoxythiophene, 2,2-bis(bromomethyl)propane-1,3-diol, p-toluenesulfonic acid (p-TSA), 2-ethylhexanoic acid, N-bromosuccinimide (NBS), palladium(II) acetate [$Pd(OAc)_2$], pivalic acid, potassium carbonate (K_2CO_3), magnesium sulfate ($MgSO_4$), sodium bicarbonate ($NaHCO_3$), and all organic solvents were purchased from Sigma-Aldrich and used as received unless otherwise stated. Dry toluene and dry N,N-dimethylacetamide (DMAc) were used for moisture-sensitive synthesis steps. Hexane, dichloromethane, ethyl acetate, diethyl ether, methanol, acetone, and chloroform were used for extraction, precipitation, column chromatography, Soxhlet purification, and polymer recovery. Deionized water was used for all aqueous washing procedures.

Synthesis of 3,3-bis(bromomethyl)-3,4-dihydro-2H-thieno[3,4-b][1,4]dioxepine.

Monomer and polymer were prepared according to a previously reported procedure with minor modification. In brief, 3,4-dimethoxythiophene (1.00 g, 6.94 mmol), 2,2-bis(bromomethyl)propane-1,3-diol (3.72 g, 14.2 mmol), and p-toluenesulfonic acid (p-TSA, 0.119 g, 0.694 mmol) were combined in dry toluene under an argon atmosphere. The reaction mixture was heated under reflux to promote the acid-catalyzed transacetalization/cyclization reaction. After the initial reaction period, an additional portion of 2,2-bis(bromomethyl)propane-1,3-diol (0.372 g, 1.42 mmol) was introduced, and the reaction was continued until completion. The mixture was then cooled to room temperature and worked up by extraction with ethyl acetate and water. The organic phase was dried over $MgSO_4$, filtered, and concentrated under reduced pressure. The crude dark residue was purified by silica gel column chromatography using a 1:1 hexanes/dichloromethane eluent to afford M4 as a pale-yellow solid.

Synthesis of ProDOT bis(2-ethylhexanoate) derivative

ProDOT(CH_2Br)$_2$ (1.00 g, 2.92 mmol, 1.0 equiv.), 2-ethylhexanoic acid (ca. 1.1 g, 7.6 mmol, 2.6 equiv.), K_2CO_3 (1.21 g, 8.76 mmol, 3.0 equiv.), and dry DMAc (ca. 28 mL) were added to a dry round-bottom flask under an argon atmosphere. The reaction mixture was heated at 100 °C overnight. After cooling to room temperature, the mixture was extracted with diethyl ether and brine. The combined organic layers were washed several times with saturated $NaHCO_3$ solution to remove residual acid, followed by washing with water. The organic phase was then dried, filtered, and concentrated under reduced pressure. The crude oily residue was purified by silica gel column chromatography, using a gradient from hexanes to 20% ethyl acetate in hexanes. After drying under high vacuum overnight, the desired product was obtained as a pale yellow oil.

Synthesis of ProDOT(EH)-Br$_2$

ProDOT(EH)$_2$, bearing 2-ethylhexanoate ester side chains, was brominated following a modified literature procedure. In a typical reaction, ProDOT(EH)$_2$ (1.00 g, approximately 2.13 mmol, 1.0 equiv.) was dissolved in dry DMAc (approximately 24 mL) under argon and cooled to 0 °C. NBS (0.84 g, 4.69 mmol, 2.2 equiv.) was added in one portion, and the reaction mixture was protected from light with aluminum foil. The mixture was stirred overnight while slowly warming to room temperature. The reaction mixture was then extracted with diethyl ether, washed with saturated $NaHCO_3$ solution and brine, and concentrated under reduced pressure. The crude product was purified by silica gel column chromatography using a gradient from

https://doi.org/10.66973/jees.26.008

hexanes to 20% ethyl acetate in hexanes. The desired dibrominated monomer, ProDOT(EH)-Br_2, was obtained as a pale-yellow oil after drying under high vacuum.

Polymerization of ProDOT(EH)-Br_2

PProDOT(EHE) was synthesized via direct heteroarylation polymerization using equimolar amounts of ProDOT(EHE) and ProDOT(EHE)-Br_2. ProDOT(EHE) (0.3572 g, 1.20 mmol, 1.0 equiv.) and ProDOT(EHE)-Br_2 (0.5461 g, 1.20 mmol, 1.0 equiv.) were initially weighed into separate vials. $Pd(OAc)_2$ (0.0052 g, 2 mol%), pivalic acid (0.0444 g, approximately 0.3 equiv.), K_2CO_3 (0.436 g, 2.5 equiv.), and a magnetic stir bar were added to a 50 mL round-bottom flask. The monomers were transferred into the flask using dry DMAc (12 mL), and the reaction mixture was degassed by argon bubbling. The flask was then placed in an oil bath at 100 °C, and the reaction was stirred vigorously overnight. After cooling to room temperature, the polymer was precipitated into stirred methanol. The precipitate was collected in a Soxhlet thimble and purified by sequential washing with methanol, acetone, ethyl acetate, and hexane, followed by extraction with $CHCl_3$. The chloroform fraction appeared as a dark magenta solution.

3 Results and Discussion

The ProDOT-based polymer was designed to combine the electroactive 3,4-propylenedioxythiophene core with flexible branched ester side chains to improve solubility, film-forming ability, and electrochromic performance. The synthetic route involved preparation of the ProDOT monomer, introduction of 2-ethylhexanoate ester side chains, bromination at the thiophene α-positions, and subsequent direct heteroarylation polymerization using Pd $(OAc)_2$, pivalic acid, and K_2CO_3 in DMAc. After purification by precipitation and Soxhlet extraction, the polymer was obtained as a pink–magenta solid. The successful formation of the target monomers and polymer was confirmed by NMR spectroscopy (Figure S (1-4)), and further structural verification was carried out by FTIR analysis.

For electrochromic measurements, both PProDOT(EHE) and PProDOT(OH) films were prepared with a comparable thickness of approximately 300 nm. Maintaining the same film thickness is important because electrochromic optical contrast and switching kinetics are strongly thickness dependent. In general, thicker films can provide higher optical density and stronger color modulation, whereas excessively thick films may limit ion diffusion and slow down switching[31], [32].

FTIR spectroscopy was used to confirm the chemical structure of the ester-functionalized polymer and to evaluate the structural changes after hydrolysis. Figure 1 shows the FTIR spectra of the unhydrolyzed PProDOT(EHE)-based polymer and the hydrolyzed PProDOT(OH)-based polymer. Both spectra display characteristic vibrational features of the poly(3,4-alkylenedioxythiophene)-type backbone, indicating that the conjugated main chain was preserved after hydrolysis. The bands observed in the fingerprint region can be assigned to thiophene ring vibrations, C–S–C deformation, C–O–C stretching of the alkylenedioxy ring, and C–H bending vibrations of the alkyl substituents. For the unhydrolyzed PProDOT(EHE)-based polymer, the presence of ester-containing side chains is supported by the characteristic carbonyl stretching vibration in the region around 1700–1750 cm^{-1}. In addition, strong absorption bands in the 1000–1300 cm^{-1} region can be attributed to C–O–C and C–O stretching vibrations arising from both the ProDOT ring and the ester/ether side-chain functionalities. The bands associated with aliphatic C–H bending and thiophene ring deformation further confirm the presence of the substituted ProDOT framework.

After hydrolysis, clear changes are observed in the FTIR spectrum of the PProDOT(OH)-based polymer. The intensity of the ester carbonyl band increases significantly, indicating the successful conversion of ester-containing side chains into hydrolyzed functional groups. At the same time, changes in the 1000–1300 cm^{-1} region suggest modification of the C–O environment after hydrolysis. The hydrolyzed polymer also shows a broad absorption feature in the high-wavenumber region, which can be associated with O–H stretching vibrations. The broad nature of

https://doi.org/10.66973/jees.26.008

this band suggests the possible formation of intermolecular hydrogen bonding between hydroxyl-containing side chains. Importantly, the characteristic vibrations of the ProDOT/thiophene backbone remain visible after hydrolysis, suggesting that the post-polymerization modification mainly affects the side-chain functionality rather than destroying the conjugated polymer backbone[33], [34]. Therefore, the FTIR results confirm the successful hydrolysis of the ester-functionalized polymer and support the formation of the hydroxyl-functionalized polymer structure. These structural changes are expected to influence the polarity, intermolecular interactions, film morphology, and electrochemical/electrochromic behavior of the polymer.

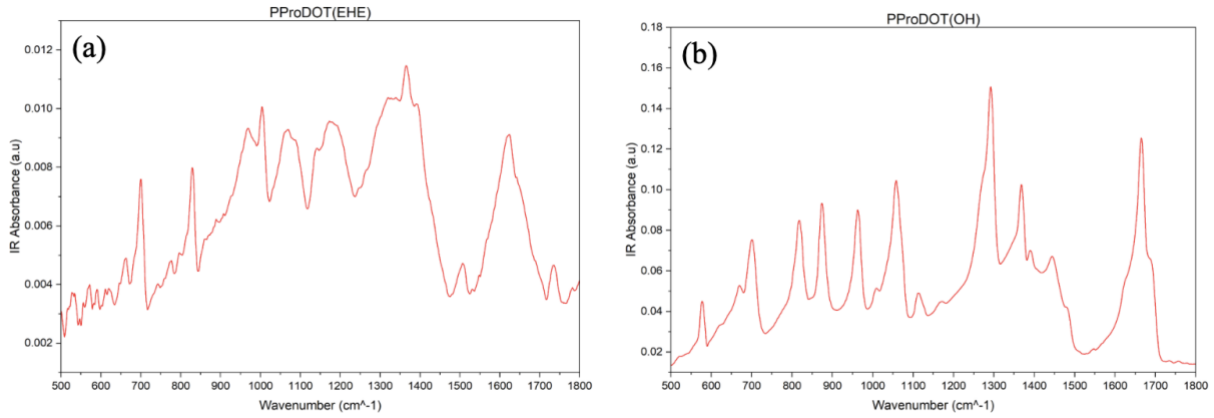

Figure 1. FTIR spectra of ProDOT-based polymers: (a) pristine PProDOT(EHE), (b) hydrolyzed PProDOT(OH).

X-ray photoelectron spectroscopy (XPS) was used to investigate the surface elemental composition and chemical-state changes of the unhydrolyzed PProDOT(EHE) and hydrolyzed PProDOT(OH) samples (Figure 2). The survey spectra of both polymers show the expected signals corresponding to C 1s, O 1s, and S 2p, confirming the presence of carbon- and oxygen-containing side chains together with the sulfur-containing thiophene/ProDOT backbone. The absence of additional intense impurity peaks indicates that the polymers were successfully purified after synthesis and post-polymerization modification.

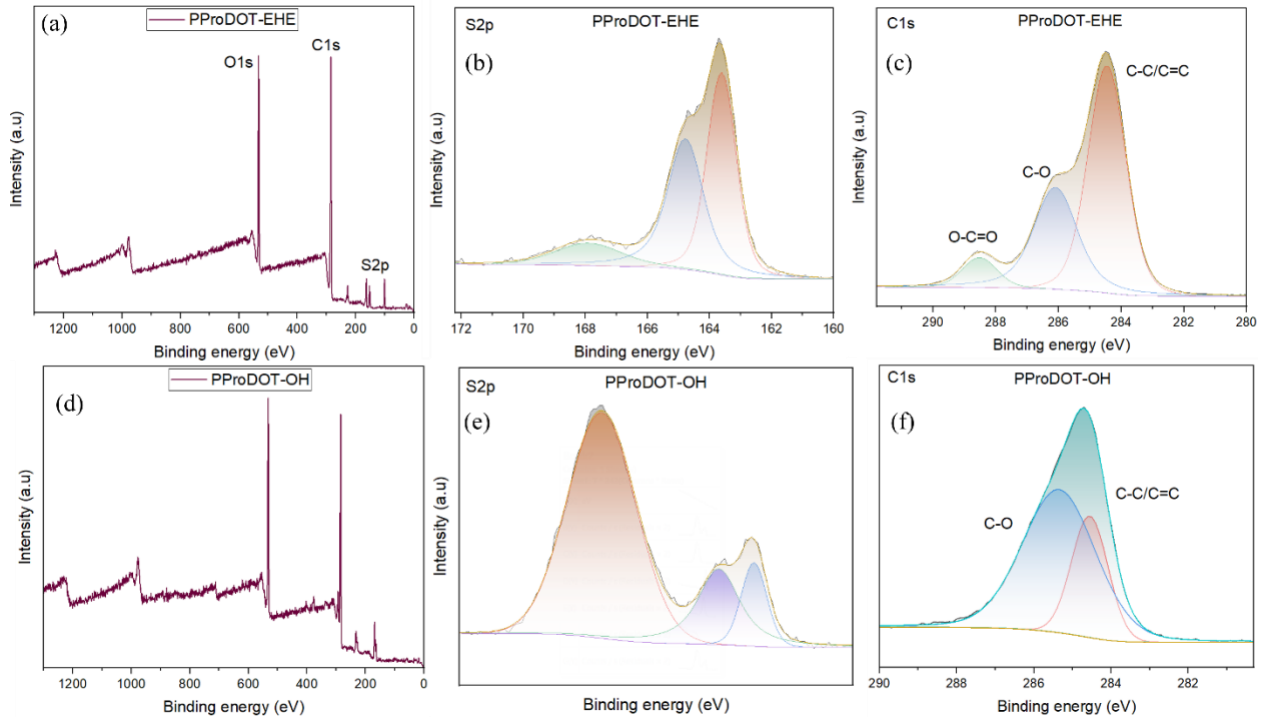

https://doi.org/10.66973/jees.26.008

Figure 2. XPS analysis of unhydrolyzed and hydrolyzed ProDOT-based polymers: survey spectrum of (a) PProDOT(EHE) and (d) PProDOT(OH); high-resolution S 2p spectra of (b) PProDOT(EHE) and (e) PProDOT(OH); and high-resolution C 1s spectra of (c) PProDOT(EHE) and (f) PProDOT(OH).

For the unhydrolyzed PProDOT(EHE) sample, the high-resolution C 1s spectrum can be deconvoluted into three main components. The dominant peak at approximately 284.5–284.8 eV is assigned to C–C/C=C bonds from the conjugated thiophene backbone and alkyl side chains. The component around 286.0–286.5 eV corresponds to C–O bonds originating from the alkylenedioxy ring and ether/ester side-chain environment. A higher binding energy contribution near 288.5–289.0 eV is attributed to O–C=O carbonyl carbon, confirming the presence of ester groups in the EHE-substituted polymer.

After hydrolysis, the C 1s spectrum of PProDOT(OH) changes significantly. The high-binding-energy O–C=O component strongly decreases or disappears, indicating successful cleavage/removal of the ester functionality. At the same time, the C–O contribution becomes more dominant, which is consistent with the formation of hydroxyl-containing side chains after hydrolysis. The main C–C/C=C component remains present in both samples, suggesting that the π-conjugated ProDOT/thiophene backbone is largely retained during the hydrolysis process. This is important because it confirms that hydrolysis modifies mainly the side-chain chemistry rather than destroying the electroactive polymer backbone[35], [36].

The high-resolution S 2p spectra were analyzed to evaluate changes in the sulfur chemical environment of the ProDOT-based polymers before and after hydrolysis. Since sulfur is in the thiophene/ProDOT backbone, the S 2p region provides useful information on the preservation of the conjugated structure and possible changes in the local oxidation state of sulfur. The relative contribution of each sulfur component was calculated from the fitted peak areas using Atotal = ΣAi and Relative contribution (%) = (Ai / A_{total}) × 100, where A_{total} is the total fitted S 2p peak area and Ai is the fitted area of an individual S 2p component.

For PProDOT-EHE, the S 2p spectrum shows a dominant peak at 163.7 eV, assigned to neutral thiophene sulfur, and a weaker high-binding-energy component at 167.8 eV, attributed to oxidized sulfur species. The calculated contributions of neutral and oxidized sulfur are 78.9% and 21.1%, respectively, indicating that sulfur in the unhydrolyzed polymer is mainly present in the neutral thiophene environment. After hydrolysis, PProDOT-OH shows a noticeable change in the S 2p profile. The neutral thiophene sulfur components appear at 163.4 and 164.7 eV, corresponding to the S $2p_{3/2}$ and S $2p_{1/2}$ spin–orbit components, while the high-binding-energy component at 168.4 eV is assigned to oxidized sulfur species. The combined neutral thiophene sulfur contribution decreases to 25.0%, whereas the oxidized sulfur contribution increases to 75.0%. This change suggests that hydrolysis affects the surface chemical environment of the polymer, possibly due to increased polarity, interaction with oxygen-containing groups, partial surface oxidation, or residual species after post-treatment. The fitted parameters and calculated relative contributions are summarized in Table S1[33], [37], [38].

The comparison between PProDOT(EHE) and PProDOT(OH) demonstrates that hydrolysis does not completely remove the thiophene sulfur signal, meaning that the conjugated ProDOT backbone is still preserved. However, the large increase in the high-binding-energy sulfur contribution after hydrolysis indicates a substantial change in the surface electronic environment of sulfur atoms.

The work function (Φ) was calculated from the UPS spectra using the kinetic-energy scale according to $\Phi = h\nu - (E_F,KE - E_{cutoff},KE)$, where hν is the photon energy, E_F,KE is the kinetic energy of the Fermi level, and Ecutoff,KE is the kinetic energy of the secondary electron cutoff[39], [40], [41]. For He I excitation, hν = 21.22 eV. For PProDOT(EHE), E_{cutoff},KE and E_F,KE were determined to be 14.02 and 30.54 eV, respectively, giving Φ = 21.22 − (30.54 − 14.02) = 4.70 eV. For PProDOT-OH, E_{cutoff},KE and E_F,KE were determined to be 13.98 and 30.89 eV, respectively, giving Φ = 21.22 − (30.89 − 13.98) = 4.31 eV

The HOMO energy level was calculated using

$$HOMO = -(\Phi + E_{onset})$$

https://doi.org/10.66973/jees.26.008

where E_{onset} is the photoemission onset energy obtained from the UPS spectrum. The LUMO energy level was estimated using

$$LUMO = HOMO + E_g$$

where E_g is the optical band gap obtained from the Tauc plot (Figure S5).

For PProDOT(EHE), the optical band gap was estimated to be 1.64 eV, whereas PProDOT(OH) showed a lower band gap of 1.43 eV. The decrease in band gap after hydrolysis suggests that the conversion of the EHE side chains into hydroxyl-containing groups affects the electronic structure of the polymer. This may be related to changes in intermolecular interactions, polymer chain packing, and conjugation efficiency in the solid state. The lower band gap of PProDOT(OH) indicates improved electronic delocalization or stronger interchain interaction compared with the unhydrolyzed polymer.

UPS analysis also shows clear differences between the two polymers (Table S2). The work function decreases from 4.70 eV for PProDOT(EHE) to 4.31 eV for PProDOT(OH). At the same time, the onset energy decreases from 1.20 eV to 0.88 eV after hydrolysis. Based on these values, the HOMO level of PProDOT(EHE) was calculated as −5.90 eV, while that of PProDOT(OH) was −5.19 eV. This upward shift of the HOMO level after hydrolysis indicates that the hydrolyzed polymer may be more easily oxidized, which is consistent with improved electrochemical activity.

The LUMO levels were estimated from the HOMO values and optical band gaps. PProDOT(EHE) exhibited a LUMO level of −4.26 eV, while PProDOT(OH) showed a LUMO level of −3.76 eV. The simultaneous shift of both HOMO and LUMO levels after hydrolysis confirms that side-chain modification strongly influences the electronic energy structure of the polymer. These results suggest that hydrolysis does not only change the chemical functionality of the side chains, but also affects the electronic properties of the conjugated backbone in the thin-film state.

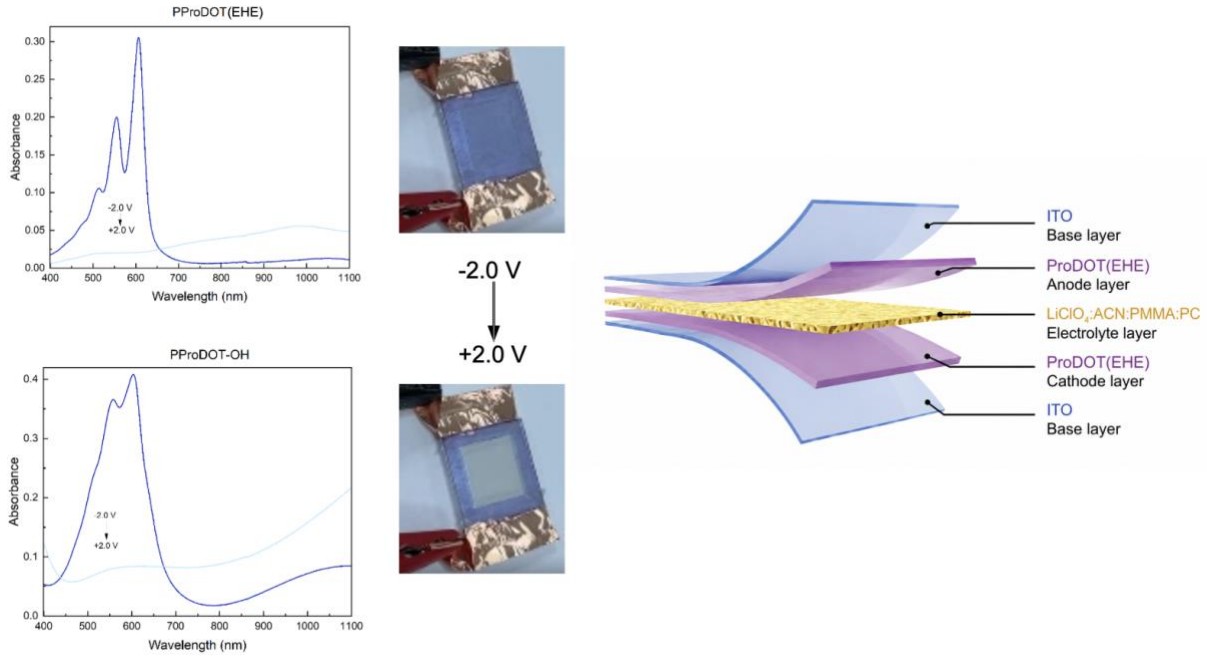

Figure 3. UV–Vis spectroelectrochemical response and device color change of PProDOT(EHE), PProDOT(OH) electrochromic devices and device architecture of the fabricated electrochromic cell.

The electrochromic behavior of PProDOT(EHE) and PProDOT(OH) was evaluated by UV–Vis spectroelectrochemistry at −2.0 and +2.0 V. Both devices show clear potential-dependent optical changes, confirming their electrochromic activity. In the neutral state, strong visible absorption bands are observed around 550–620 nm, corresponding to π–π* transitions of the conjugated ProDOT backbone. Upon oxidation, the visible absorption decreases, while broad absorption in the longer-wavelength

https://doi.org/10.66973/jees.26.008

region increases, indicating the formation of polaronic/bipolaronic charge carriers. Compared with PProDOT(EHE), PProDOT(OH) shows stronger spectral modulation, which may result from improved interaction between the hydroxyl-functionalized polymer and the PMMA gel electrolyte (Figure 3). The photographs further confirm visible color switching in the assembled devices.

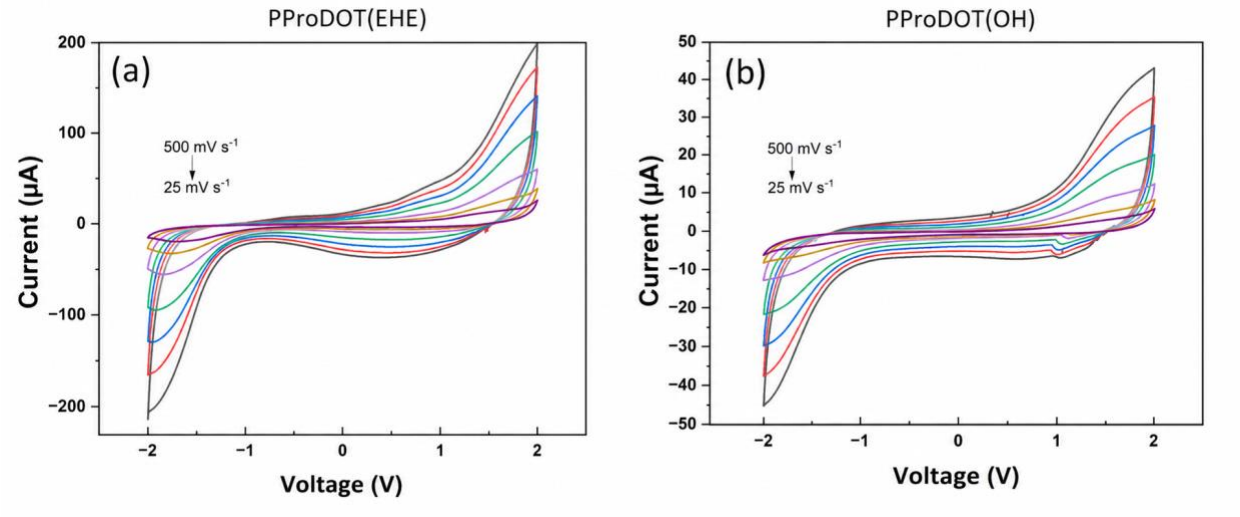

Figure 4. Cyclic voltammograms of (a) PProDOT(EHE) and (b) PProDOT(OH) recorded at different scan rates from 25 to 500 mV s^{-1}.

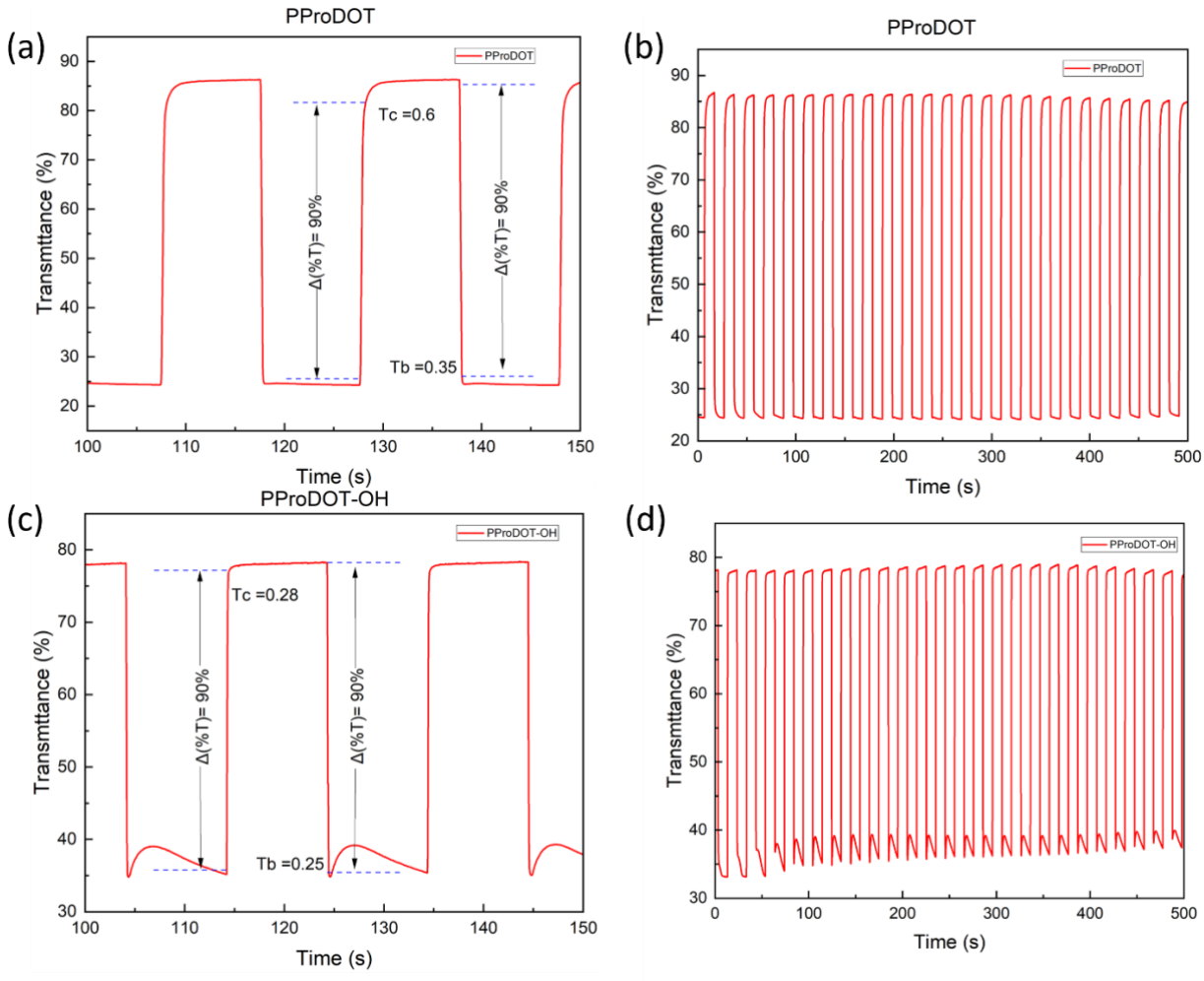

https://doi.org/10.66973/jees.26.008

Figure 5. Optical switching and cycling stability of PProDOT(EHE) and PProDOT(OH) electrochromic devices: response-time analysis of (a) PProDOT(EHE) and (c) PProDOT(OH), and repeated transmittance switching profiles of (b) PProDOT(EHE) and (d) PProDOT(OH) under alternating applied potentials.

The electrochemical behavior of PProDOT(EHE) and PProDOT(OH) was investigated by cyclic voltammetry at scan rates from 25 to 500 mV s^{-1} (Figure 4). Both polymers show clear redox activity within the applied potential window, confirming the electroactive nature of the ProDOT-based conjugated backbone. As the scan rate increases, the anodic and cathodic current responses increase, indicating faster charge transfer and ion movement during the doping/dedoping process.

Compared with PProDOT(EHE), the PProDOT(OH) sample shows lower current intensity, suggesting that hydrolysis affects the electrochemical response of the polymer film. This difference may be related to changes in film morphology, polarity, thickness, or ion transport after conversion of the ester-containing side chains into hydroxyl-containing groups. The retained redox behavior of PProDOT(OH) confirms that the conjugated backbone remains electrochemically active after hydrolysis.

The dynamic electrochromic switching behavior of PProDOT(EHE) and PProDOT(OH) was evaluated by monitoring the transmittance change as a function of time under repeated potential switching. Both polymers exhibit clear and reversible optical modulation, confirming their ability to switch between colored and bleached states in the device configuration.

For PProDOT(EHE), the transmittance changes sharply between approximately 25% and 85%, giving a high optical contrast of about 60% (Figure 5). The coloration and bleaching processes are fast, with estimated response times of Tc = 0.6 s and Tb = 0.35 s, respectively. This indicates efficient redox switching and rapid ion transport within the polymer/electrolyte interface.

For PProDOT(OH), the device also shows reversible switching, with transmittance changing between approximately 35% and 78%. Although the optical contrast is slightly lower than that of PProDOT(EHE), the response is faster, with Tc = 0.28 s and Tb = 0.25 s. The faster switching of PProDOT(OH) may be attributed to the hydroxyl-functionalized side chains, which increase polymer polarity and improve interaction with the PMMA gel electrolyte. This can facilitate ion penetration and charge compensation during the doping/dedoping process.

The long-term switching curves further demonstrate the cycling stability of both devices over repeated operation. PProDOT(EHE) maintains a large and stable transmittance window over multiple cycles, while PProDOT(OH) shows slightly smaller but highly reproducible switching behavior. The stable periodic response indicates that both polymer films tolerate repeated redox cycling without severe degradation during the tested period.

The electrochromic performance of PProDOT(EHE) and PProDOT(OH) was compared with previously reported ProDOT-based materials, as summarized in Table 1. The present PProDOT(EHE) device shows a switching time of 0.6/0.35 s, an optical contrast of 61.99%, and a high coloration efficiency of 872.2 cm^2 C^{-1}. These values indicate that PProDOT(EHE) exhibits fast switching, strong optical modulation, and efficient charge utilization compared with many reported ProDOT derivatives.

The hydrolyzed PProDOT(OH) sample shows even faster switching behavior, with coloration and bleaching times of 0.28/0.25 s. Although its optical contrast is lower (43.41%) than that of PProDOT(EHE), its coloration efficiency remains high at 599 cm^2 C^{-1}. This suggests that hydrolysis improves the switching kinetics, likely due to enhanced polymer–electrolyte interaction and faster ion transport through the hydroxyl-functionalized polymer film.

https://doi.org/10.66973/jees.26.008

Table 1. Comparison of electrochromic performance of PProDOT(EHE) and PProDOT(OH) with previously reported ProDOT-based electrochromic materials.

Material	Switching time (s)	CE ($cm^2\ C^{-1}$)	Optical contrast (ΔT)	Ref.
PProDOTs	2	-	70 %	[41]
PProDOT(Me)$_2$	~0.7	NR	60 %	[4]
P(ProDOT-ester)	0.3 / 3.7	123	27.7 %	[4]
Homopolymer ProDOT	1.8	-	56 %	[42]
OSProZ	0.64 s/0.47 s	598	66.4 %	[7]
ProDOT-sultone	1.2 s	250	40 %	[43]
PProDOT(EHE)	0.6/0.35	872.2	61.99 %	Present work
PProDOT(OH)	0.28/0.25	599	43.41 %	Present work

Conclusion

In summary, ester-functionalized PProDOT(EHE) and hydrolyzed PProDOT(OH) were successfully prepared and investigated as electrochromic conducting polymers. Structural characterization confirmed that hydrolysis modified the side-chain functionality while preserving the ProDOT-based conjugated backbone. FTIR analysis showed clear changes in the ester- and C–O-related vibrational regions after hydrolysis, while the XPS C 1s spectra confirmed a decrease in the ester-related O–C=O contribution and an increased presence of C–O environments. S 2p XPS analysis further demonstrated that thiophene sulfur remained present in both polymers, supporting retention of the sulfur-containing conjugated backbone, although hydrolysis produced a significant change in the surface sulfur environment.

Optical and UPS analyses revealed that side-chain hydrolysis strongly influenced the electronic structure of the polymer. The optical band gap decreased from 1.64 eV for PProDOT(EHE) to 1.43 eV for PProDOT(OH), while the HOMO level shifted from −5.90 to −5.19 eV. These changes suggest that hydrolysis modifies electronic delocalization and/or interchain interactions in the solid state. Cyclic voltammetry confirmed that both polymers remained electrochemically active, demonstrating that the hydrolysis process did not destroy the electroactive backbone.

Electrochromic device measurements using a PMMA gel electrolyte showed clear and reversible optical switching for both polymers. PProDOT(EHE) exhibited a higher optical contrast of 61.99% and a high coloration efficiency of 872.2 $cm^2\ C^{-1}$, indicating strong optical modulation and efficient charge utilization. In contrast, PProDOT(OH) showed faster switching behavior, with coloration and bleaching times of 0.28 and 0.25 s, respectively, while maintaining a good coloration efficiency of 599 $cm^2\ C^{-1}$. This difference suggests that the hydroxyl-functionalized side chains enhance polymer–electrolyte interactions and facilitate faster ion transport during redox switching.

Author Contributions

A.T.: investigation, data collection, formal analysis. S.A.: electrochemical/electrochromic measurements, data analysis. A.Z.: XPS/UPS analysis, material characterization, data interpretation. D.K.: conceptualization, methodology, supervision, writing and editing, corresponding author. M.K.: validation, scientific discussion. S.A.: supervision, writing and editing.

Funding

This work was supported by the Ministry of Science and Higher Education of the Republic of Kazakhstan under Grant No. AP27510617.

Conflict of Interest

Authors declare they have no known conflict of interest

Data availability

All required data will be available upon request from the corresponding authors.

Ethics Approval and Consent to Participate

This study did not involve human participants or animals. Therefore, ethical approval and informed consent were not required.

AI Use Disclosure

No AI tools were used to generate scientific results, data, figures, or interpretations. All analyses, conclusions, and scientific content were developed by the authors.

REFERENCES

[1] J. Chen, G. Song, S. Cong, and Z. Zhao, "Resonant-Cavity-Enhanced Electrochromic Materials and Devices," Nov. 23, 2023, *John Wiley and Sons Inc*. doi: 10.1002/adma.202300179.

[2] C. Gu, A. B. Jia, Y. M. Zhang, and S. X. A. Zhang, "Emerging Electrochromic Materials and Devices for Future Displays," Sep. 28, 2022, *American Chemical Society*. doi: 10.1021/acs.chemrev.1c01055.

[3] D. Chen *et al.*, "Multifunctional electrochromic materials and devices recent advances and future potential," Jan. 01, 2025, *Elsevier B.V.* doi: 10.1016/j.cej.2024.157820.

[4] D. Tang *et al.*, "A Highly Efficient and Energy Saving Electrochromic Platform for Adaptive Visible and Near-Infrared Light Modulation," *Chemical Engineering Journal*, vol. 482, Feb. 2024, doi: 10.1016/j.cej.2024.148870.

[5] G. Kuang, H. Yin, C. Li, Y. Tao, Y. Guo, and S. Zhang, "Developing conjugated polymers with broad-band absorption covering visible and near-infrared regions for electrochromism," *Polym. Chem.*, vol. 16, no. 15, pp. 1659–1668, Mar. 2025, doi: 10.1039/d4py01461h.

[6] A. M. M. Hasan *et al.*, "Rapid Cathodic Coloration in Solution-Processable Electrochromic Polymers of Intrinsic Microporosity," *J. Am. Chem. Soc.*, May 2025, doi: 10.1021/jacs.5c02014.

[7] H. Miao, L. Chen, F. Xing, H. Li, T. Baumgartner, and X. He, "Viologen-based solution-processable ionic porous polymers for electrochromic applications," *Chem. Sci.*, vol. 15, no. 20, pp. 7576–7585, Apr. 2024, doi: 10.1039/d4sc01408a.

[8] S. Yan, L. Zhang, X. Lv, J. Sun, Y. Zhang, and C. Zhang, "Black-to-Transmissive Electrochromism in π-Conjugated Polymer-Based Materials and Devices," *Adv. Photonics Res.*, vol. 3, no. 1, Jan. 2022, doi: 10.1002/adpr.202000199.

[9] K. Lin *et al.*, "Electrochromic conjugated polymers: The relationship of gradient band gap and electrochromic performance," *Dyes and Pigments*, vol. 232, Jan. 2025, doi: 10.1016/j.dyepig.2024.112504.

[10] V. H. R. Souza, A. Schmidt, and A. J. G. Zarbin, "A tunable color palette of electrochromic materials achieved through an ingenious stacking of ordinary conducting polymers," *J. Mater. Chem. A Mater.*, vol. 11, no. 35, pp. 18853–18861, Aug. 2023, doi: 10.1039/d3ta02860g.

[11] M. Yaseen *et al.*, "State-of-the-art electrochromic thin films devices, fabrication techniques and applications: a review," 2023, *Taylor and Francis Ltd.* doi: 10.1080/20550324.2023.2291619.

[12] K. Foroutani *et al.*, "Conducting Polymer-Based Coatings and Thin Films: A Review on Film Processing and Deposition Techniques," 2025, *Taylor and Francis Ltd.* doi: 10.1080/15583724.2025.2511828.

[13] K. Lin *et al.*, "Toward High-Performance Electrochromic Conjugated Polymers: Influence of Local Chemical Environment and Side-Chain Engineering," *Molecules*, vol. 27, no. 23, Dec. 2022, doi: 10.3390/molecules27238424.

[14] Y. Cai *et al.*, "High-Performance Electrochromic Polymers Enabled by Side-Chain Engineering for Intelligent Windows and Supercapacitors," *Eur. Polym. J.*, vol. 228, Mar. 2025, doi: 10.1016/j.eurpolymj.2025.113796.
[15] R. Kedia, M. Balkhandia, M. Khatak, N. Chaudhary, and A. Patra, "Electrochemical, optical and electrochromic properties of fused polydithienothiophene: A stable material with reversible doping," *Synth. Met.*, vol. 299, Nov. 2023, doi: 10.1016/j.synthmet.2023.117478.
[16] P. Rout, P. Mehra, W. J. Lee, L. You, and J. Mei, "Voltage-Gated Dedoping of n-Doped Poly(benzodifurandione) as an Interfacial Protective Mechanism in Electrochromic Devices," *Adv. Funct. Mater.*, May 2026, doi: 10.1002/adfm.202531933.
[17] R. Zhang *et al.*, "Composite Film of Cellulose and PEDOT:PSS for Sustainable and Stable Electrochromic Materials," *ACS Appl. Bio Mater.*, vol. 8, no. 11, pp. 10344–10351, Nov. 2025, doi: 10.1021/acsabm.5c01648.
[18] W. Liu *et al.*, "Harnessing the spectrum: High-performance infrared electrochromic device with multicolor visibility based on PEDOT:PSS/SWCNT films," *Chemical Engineering Journal*, vol. 527, Jan. 2026, doi: 10.1016/j.cej.2025.171638.
[19] L. Cao *et al.*, "A dual-functional PEDOT-based electrochromic supercapacitor with excellent electrochemical stability," *J. Power Sources*, vol. 657, Nov. 2025, doi: 10.1016/j.jpowsour.2025.238186.
[20] H. Cai *et al.*, "Progress in Conducting Polymers: Synthesis, Stability, and Ionic/Electronic Transport Properties," Mar. 27, 2026, *John Wiley and Sons Inc*. doi: 10.1002/cssc.202501277.
[21] J. F. Ponder *et al.*, "Oligoether-Functionalized PEDOT: Combining an EDOT Backbone with Polar Side Chains for Solution Processability and High Electrical Conductivity," Apr. 06, 2026, *American Chemical Society*. doi: 10.1021/acsmaterialslett.5c01567.
[22] J. Liu *et al.*, "N, P-doped carbon spheres wrapped with PProDOT and CoNi-LDH nanosheets for supercapacitor electrodes," *Chemical Engineering Journal*, vol. 533, Apr. 2026, doi: 10.1016/j.cej.2026.174839.
[23] Y. Zhou *et al.*, "Ultrasensitive label-free optical recording of bioelectric potentials using dioxythiophene-based electrochromic polymers," *Nature Communications* , vol. 16, no. 1, Dec. 2025, doi: 10.1038/s41467-025-61708-y.
[24] T. Zubair, R. S. Ramos, A. Morales, and R. M. Pankow, "Synthesis of poly(3,4-propylenedioxythiophene) (PProDOT) analogues via mechanochemical oxidative polymerization," *Polym. Chem.*, vol. 16, no. 10, pp. 1188–1196, Jan. 2025, doi: 10.1039/d4py01253d.
[25] K. Lin *et al.*, "Truxene-based multisite-polymerized electrochromic polymers: Multicolor variation, excellent cycling stability, and flexible devices," *Solar Energy Materials and Solar Cells*, vol. 293, Dec. 2025, doi: 10.1016/j.solmat.2025.113871.
[26] A. E. Bejan, C. P. Constantin, A. Nicolescu, and M. D. Damaceanu, "ProDOT conjugated polymer-powered electrode materials: From rigid to flexible electrochromic supercapacitors," *Chemical Engineering Journal*, vol. 532, Mar. 2026, doi: 10.1016/j.cej.2026.174223.
[27] M. Khatak, M. Balkhandia, R. Kedia, and A. Patra, "Pathways to Functional Polymers: Chemically versus Electrochemically Synthesized Polypropylenedioxythiophene Derivatives," *ACS Appl. Polym. Mater.*, vol. 7, no. 15, pp. 10016–10025, Jul. 2025, doi: 10.1021/acsapm.5c01705.
[28] F. A. Bravo-Plascencia, M. P. Flores-Morales, A. Kuhn, G. Salinas, and B. A. Frontana-Uribe, "Fundamental concepts of 3,4-alkoxythiophene-based polymeric systems, from synthesis to applications," Aug. 26, 2025, *Royal Society of Chemistry*. doi: 10.1039/d5ta03149d.
[29] Y. Guan *et al.*, "Reconstructing reaction kinetics via charge transfer complexes of polyaniline and TCBQ for high performance supercapacitors and electrochromic devices," *Energy*, vol. 360, Sep. 2026, doi: 10.1016/j.energy.2026.141432.
[30] K. Feng *et al.*, "The underestimated potential of amorphous covalent organic polymers in electrochromism and energy storage," *Chemical Engineering Journal*, vol. 524, Nov. 2025, doi: 10.1016/j.cej.2025.169141.
[31] Z. Wang, L. You, V. Pandit, J. Chaudhary, W. J. Lee, and J. Mei, "Transparent Electrochromic Polymers with High Optical Contrast and Contrast Ratio," *JACS Au*, vol. 4, no. 6, pp. 2291–2299, Jun. 2024, doi: 10.1021/jacsau.4c00254.
[32] R. Brooke, J. Edberg, D. Iandolo, M. Berggren, X. Crispin, and I. Engquist, "Controlling the electrochromic properties of conductive polymers using UV-light," *J. Mater. Chem. C Mater.*, vol. 6, no. 17, pp. 4663–4670, 2018, doi: 10.1039/c7tc05833k.
[33] J. F. Ponder *et al.*, "Significant Enhancement of the Electrical Conductivity of Conjugated Polymers by Post-Processing Side Chain Removal," *J. Am. Chem. Soc.*, vol. 144, no. 3, pp. 1351–1360, Jan. 2022, doi: 10.1021/jacs.1c11558.
[34] J. F. Ponder *et al.*, "Metal-like Charge Transport in PEDOT(OH) Films by Post-processing Side Chain Removal from a Soluble Precursor Polymer," *Angew. Chem. Int. Ed.*, vol. 62, no. 1, Jan. 2023, doi: 10.1002/anie.202211600.
[35] N. Sawut *et al.*, "Enhanced electrocatalytic performance of hydroxyl-grafted PProDOT:PSS/YRFC/Pt composites for direct alcohol fuel cells," *Electrochim. Acta*, vol. 403, Jan. 2022, doi: 10.1016/j.electacta.2021.139724.

[36] V. Sethumadhavan, R. Mahjoub, K. Zuber, N. Stanford, and D. Evans, "Oxygenation of conducting polymers facilitated by structure-breaking anions," *Journal of Polymer Science*, vol. 59, no. 9, pp. 745–753, May 2021, doi: 10.1002/pol.20210095.

[37] V. Sethumadhavan, R. Mahjoub, K. Zuber, N. Stanford, and D. Evans, "Oxygenation of conducting polymers facilitated by structure-breaking anions," *Journal of Polymer Science*, vol. 59, no. 9, pp. 745–753, May 2021, doi: 10.1002/pol.20210095.

[38] S. Mahato, "Composition analysis of two different PEDOT:PSS commercial products used as an interface layer in Au/n-Si Schottky diode," *RSC Adv.*, vol. 7, no. 74, pp. 47125–47131, 2017, doi: 10.1039/c7ra10018c.

[39] Y. Nakayama, S. Kera, and N. Ueno, "Photoelectron spectroscopy on single crystals of organic semiconductors: Experimental electronic band structure for optoelectronic properties," Jul. 21, 2020, *Royal Society of Chemistry*. doi: 10.1039/d0tc00891e.

[40] T. Schultz, P. Amsalem, N. B. Kotadiya, T. Lenz, P. W. M. Blom, and N. Koch, "Importance of Substrate Work Function Homogeneity for Reliable Ionization Energy Determination by Photoelectron Spectroscopy," *Phys. Status Solidi B Basic Res.*, vol. 256, no. 2, Feb. 2019, doi: 10.1002/pssb.201800299.

[41] N. Chen, D. Wang, J. Hu, L. Guan, and Z. H. Lu, "Measuring Energy Gaps of Organic Semiconductors by Electron Energy Loss Spectroscopies," *Phys. Status Solidi B Basic Res.*, vol. 259, no. 1, Jan. 2022, doi: 10.1002/pssb.202100459.